The Relationship Between Glabellar Contraction Patterns and Glabellar Muscle Anatomy: A Magnetic Resonance Imaging–based Study

Aesthetic Surgery Journal
2024, Vol 00(0) 1–8
Editorial Decision date: September 18, 2024;
online publish-ahead-of-print October 1, 2024.

https://doi.org/10.1093/asj/sjae202
www.aestheticsurgeryjournal.com

OXFORD
UNIVERSITY PRESS

Daniel J. Rams, MD; Mateusz Koziej, MD, PhD, DSc; Jeremy B. Green, MD; Brian S. Biesman, MD; Elżbieta Szczepanek, MD; Tadeusz J. Popiela, MD, PhD; Monika Ostrogórska, PhD; Agnieszka Gleń, MD; Rod J. Rohrich, MD; Michael Alfertshofer, MD; and Sebastian Cotofana, MD, PhD

Abstract

Background: Glabellar contraction patterns were introduced to the scientific literature to help guide glabellar neuromodulator injection algorithms. However, the relationship between the underlying musculature and its influence on these glabellar contraction patterns is unclear.

Objectives: The aim of this study was to identify by magnetic resonance imaging (MRI) glabellar muscle parameters that display an influence on the distribution of individual glabellar contraction patterns.

Methods: Thirty-four healthy young individuals of Caucasian Polish descent were investigated (17 females, 17 males) with a mean age of 23.6 years and a mean BMI of 22.8 kg/m^2. MRI-based measurements of length, thickness, width, and surface area of procerus, corrugator supercilii, orbicularis oculi, and frontalis muscles were conducted.

Results: Unadjusted models revealed that there was no statistically significant difference between the 5 glabellar contraction types and the investigated muscle parameters, indicating that, independent of the skin rhytid pattern, the underlying musculature was not different between the investigated groups in this sample, with all $P \geq .102$. Adjusted models revealed that sex was the most influential factor, with males generally displaying higher values for the investigated parameters than females.

Conclusions: The results of this study reveal that, based on the MRI parameters investigated and the investigated cohort, there does not appear to be a strong relationship between glabellar contraction patterns and underlying glabella muscle anatomy. Utilizing glabellar contraction patterns to design neuromodulator treatment algorithms may be of variable clinical merit.

Level of Evidence: 3 (Therapeutic)

The number of neuromodulator treatments conducted in the US has substantially risen, 24% from 2021 to 2022, and 73% from 2019 to 2022, according to The Aesthetic Society and the American Society of Plastic Surgeons, respectively.[1,2] Of the various facial regions targeted with FDA-approved botulinum toxin products, the upper face is the most frequently requested region for neuromodulator treatments and includes horizontal forehead lines, glabellar frown lines, and lateral canthal lines.

A recent survey-based study identified that the forehead is considered by injectors 1 of the top 3 most difficult facial regions to treat with neuromodulators, although the glabella is considered the easiest facial region to address with toxins.[3] This discrepancy can best be explained by understanding the functional anatomy behind the eyebrow: the frontalis muscle (FM) is the sole eyebrow elevator, and its muscular action is opposed by the muscles of the glabellar complex

Dr Rams is a physician, Dr Koziej is a plastic surgeon, and Dr Szczepanek is an ENT surgeon, Department of Anatomy, Jagiellonian University Medical College, Kraków, Poland. Dr Green is a dermatologist in private practice in Coral Gables, FL. Dr Biesman is an oculoplastic surgeon in private practice in Nashville, TN. Dr Popiela is a professor, Dr Ostrogórska is an MRI specialist, and Dr Gleń is a radiologist, Department of Radiology, Jagiellonian University Medical College, Kraków, Poland. Dr Rohrich is a plastic surgeon in private practice in Dallas, TX. Dr Alfertshofer is a physician, Department of Oromaxillofacial Surgery, Ludwig-Maximilians-University Munich, Munich, Germany. Dr Cotofana is a professor, Department of Dermatology, Erasmus University Medical Center, Rotterdam, the Netherlands.

Corresponding Author:
Dr Sebastian Cotofana, Department of Dermatology, Erasmus Medical Center, Dr. Molewaterplein 40, 3015 GD Rotterdam, the Netherlands.
E-mail: scotofana24@gmail.com; Instagram: @professorsebastiancotofana

(corrugator supercilii [CSM], procerus [PM], orbicularis oculi muscles [OOM]), which together are considered eyebrow depressors.[4]

De Almeida et al suggested in a double publication released in 2010 and 2012 classifying patients by 5 different glabellar contraction patterns and adjusting an FDA-approved injection algorithm to the individual skin rhytid pattern for each glabellar contraction type.[5] The authors contended that an observed glabellar skin wrinkle pattern was influenced by anatomic variations in muscle morphology (including muscle activity and recruitment), among other factors such as sex, age, ethnicity, and environmental factors (eg, sun exposure, BMI).[5] Consequently, according to the authors, the glabellar injection algorithm should be adapted to address the variable glabellar muscle anatomy and optimize toxin treatment outcomes.

Subsequent publications evaluated whether this injection strategy was generalizable to other ethnicities. In 2014 Kim et al reviewed the glabellar contraction pattern proposed by de Almeida et al and the suggested adjustments in the neuromodulator injection algorithm and "found the former classification somewhat confusing" when applied to a Korean study population of 139 patients.[6] Similar feedback was provided by Kamat et al, who stated that the classification by de Almeida et al "was found to be confusing by many practitioners" when an Indian study population of 200 patients was investigated.[7] Additional discrepancies (especially in the frequency of each subtype) were noted when a Chinese population was investigated by Jiang et al in a sample of 456 and by Hsieh et al in a sample of 489 patients.[8,9]

Given the inconsistencies identified among glabellar contraction patterns across different ethnicities and the dearth of information regarding the underlying glabellar musculature contributing to these skin surface patterns, the present study was designed. The research question posed was whether variations in glabellar muscular anatomy exist, and if they do what their contribution is to each of the proposed glabellar contraction pattern types initially suggested by de Almeida et al. It can be argued that despite the existence of interindividual differences in glabellar muscular anatomy their contribution to a different skin rhytid pattern is limited. Therefore, minimal to no alterations to the FDA-approved injection algorithm are necessary. To address this question, a study sample of young, healthy, toxin-naive patients was recruited, and factors including sex, age, BMI, and various parameters (length, width, thickness, etc) of the glabellar muscles were collected and statistically analyzed. It was hoped that the results of this study would provide more insight into the relationship of glabellar skin rhytids and contraction patterns with the underlying musculature and how these findings might be clinically relevant to neuromodulator treatments.

METHODS

Study Population

In this observational magnetic resonance imaging (MRI)–based study we investigated the glabellar muscles of young healthy neuromodulator-naive volunteers between March 2022 and July 2024. Parts of this investigation have been published previously by Rams et al.[10] The study received ethics committee approval by the Jagiellonian University Ethics Committee in Krakow, Poland, under registration number NO 1072.6120.209.2022. Each participant provided written informed consent, endorsing their enrollment in the study and the utilization of their demographic and imaging-related data.

Beyond an age of 18 to 30 years old, no specific inclusion criteria were applied, to allow for a wide range of community-based MRI data sets. Exclusion criteria encompassed individuals with a BMI <18.5 or >27.99 kg/m^2, contraindications to undergoing MRI (eg, metal implants), current connective tissue diseases (eg, collagenosis), or a history of facial injuries or facial aesthetic procedures that could influence the visibility of the upper facial musculature during MRI. The last exclusion was applied to assure that the imaged muscles were captured in their physiologic state without alterations from surgical or nonsurgical interventions. Such changes to the upper facial musculature could influence their visibility and the measurements conducted.

Glabellar Contraction Pattern

Before initiating the MRI scanning procedures, patients were asked to maximally frown and thereby contract the glabellar muscles (PM, CSM, OOM, and FM). The resulting skin surface wrinkle pattern was classified according to previous publications by D.J.R. and M.K.: U-shaped, V-shaped, converging arrows, omega, and inverted omega.[5]

MR Imaging Sequence

MR imaging data were acquired with a 1.5T Siemens Magnetom Sola MR System with a 32-channel head coil (Siemens Healthcare GmbH, Erlangen, Germany). A custom T1 MPRAGE sequence was performed with the following parameters: TR = 2340 ms, TE = 5.1 ms, TI = 1180 ms, FA = 8°, FOV = 240 × 240 mm, slice thickness = 0.9 mm, 288 axial slices. Patients were asked to have a relaxed facial expression during the scanning procedure to allow for accurate recording of the muscles in repose.

MR Image Analysis

Following MR image quality completion, DICOM data sets were evaluated by 2 radiological operators with at least 10 years of dedicated experience in head and neck imaging, applying the multiplanar mode for image reconstruction in all 3 axes and the standardized radiology workstation (syngo.via software, Siemens AG, Germany). All measurements were repeated twice, and each side counted separately. The following measurements were manually conducted (Figure 1):

Procerus Muscle (PM)

1. Length of the PM = maximal vertical linear distance between the origin of the muscle at its most inferior point at the nasal bone and its fusion with the frontalis muscle
2. Width of the PM = maximal horizontal linear distance measured at reference point halfway between the nasion and a horizontal line at the upper margin of the eyebrow cilia
3. Thickness of the PM = maximal anteroposterior dimension measured at reference point halfway between the nasion and a horizontal line at the upper margin of the eyebrow cilia

Corrugator Supercilii Muscle (CSM)

1. Length of the CSM = maximal linear distance from the muscle's medial bony origin to its lateral dermal insertion near the midpupillary line
2. Width of the CSM = average vertical linear distance from the inferior to the superior border of the muscle (based on measurements obtained in each equal third)
3. Thickness of the CSM = average linear distance from the most anterior to the most posterior surface, perpendicular to the long axis of the muscle (based on measurements obtained in each equal third)

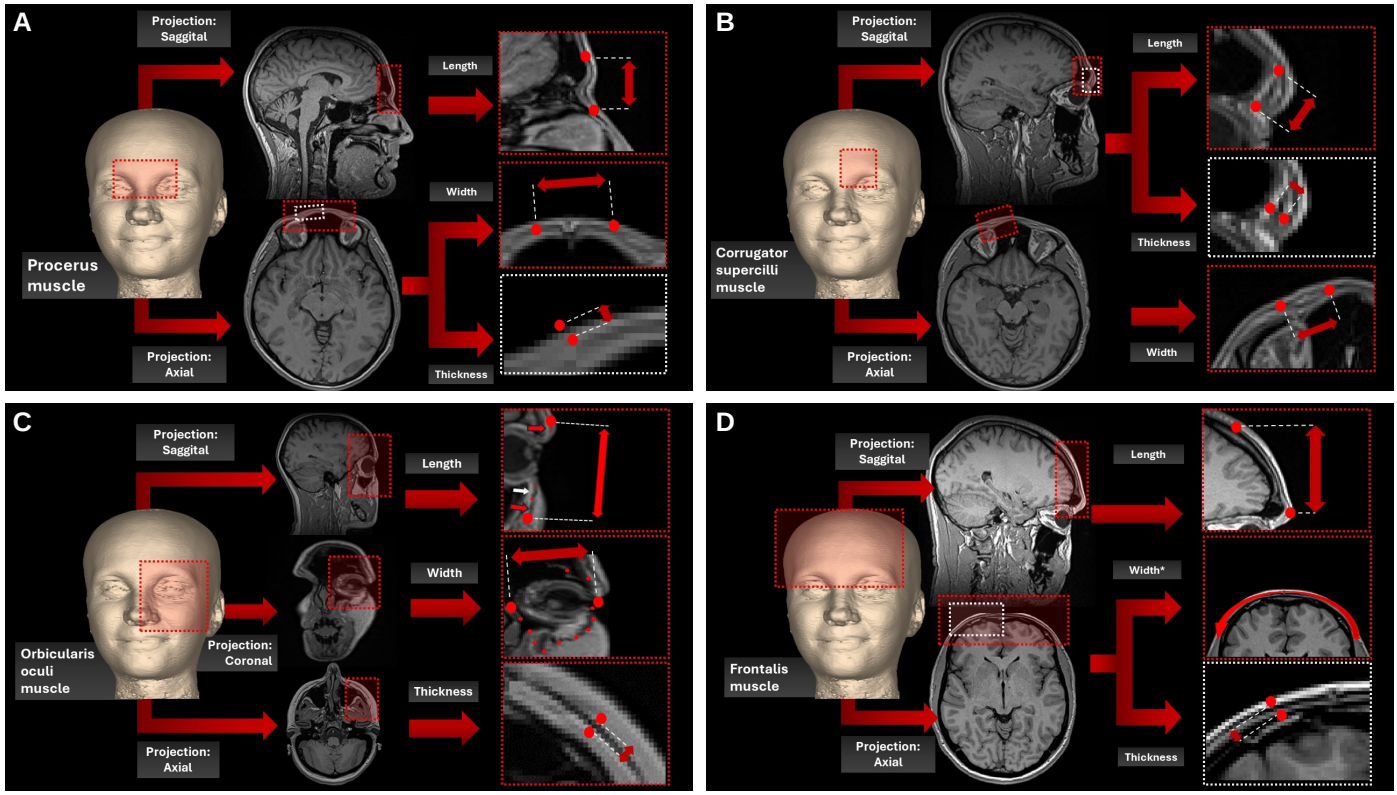

Figure 1. (A) Magnetic resonance imaging (MRI) displaying the measurement methodology for length, width, and thickness of the procerus muscle (PM). Red and white squares indicate the area of measurement. (B) MRI displaying the measurement methodology for length, width, and thickness of the corrugator supercilii muscle (CSM). Red and white squares indicate the area of measurement. (C) MRI displaying the measurement methodology for height, width, and thickness of the orbicularis oculi muscle (OOM). Red and white squares indicate the area of measurement. (D) MRI displaying the measurement methodology for length, width, and thickness of the frontalis muscle (FM). Red and white squares indicate the area of measurement.

Orbicularis Oculi Muscle (OOM)

1. Surface area of the OOM = best-fit area determined by approximating the elliptical shape from the given points corresponding to the boundaries of the muscle
2. Height of the OOM = maximal vertical linear distance from the most caudal border of the muscle in the midface to the upper border before fusion with frontalis muscle
3. Width of the OOM = maximal horizontal linear distance from the most medial border of the muscle to the most lateral border measured in the horizontal midpupillary line
4. Thickness of the OOM = average distance between its most anterior and most posterior surface (based on reference points in each quadrant of the muscle)

Frontalis Muscle (FM)

1. Length of the FM = maximal vertical distance between the upper margin of eyebrow cilia to the transition into the galea aponeurotica measured bilaterally in the vertical midpupillary line
2. Width of the FM = maximal horizontal distance between the most lateral (= temporal) muscle margins, measured 1.5 cm cranial to the bony supraciliary arch
3. Thickness of the FM = average anteroposterior distance measured 1.5 cm cranial to the bony supraciliary arch

The decision to select length, width, and thickness of a muscle instead of origin and insertion was based on the fact that such parameters are more likely to capture a muscle's "active" contractile behavior instead of the "static" or "rigid" parameters that describe a muscle's connection to bone or skin.

Reliability Analyses

To ensure MRI muscle parameter measurement consistency, a set of parameters was measured twice by the MRI analysts, and the agreement between the initial and the repeated measurement was determined by the intraclass correlation coefficient (ICC). For all measurements, the ICC was calculated to be 1.00, which has been defined as excellent reliability.

Statistical Analysis

The analytic strategy of this study was to classify the study participants into 5 glabellar contraction pattern subgroups and to identify which of the collected variables best predicted the distribution of each subgroup pattern. To do so, multinomial logistic regression models were calculated with the inclusion of age, sex, and BMI as covariates; not more than 4 covariates were allowed per calculation step so as not to underpower the model. All tests were run with SPSS 27 (IBM, Armonk, NY) and results are presented as the mean value and the respective standard deviation (SD). All variables except PM thickness, CSM thickness, and OOM thickness were normally distributed with the Shapiro-Wilk test $P > .05$, and therefore either a *t* test or Mann Witney U-test was performed to compute sex differences. Additionally, nonadjusted testing was conducted with 1-way analysis of variance (ANOVA) to identify across-group differences. Data

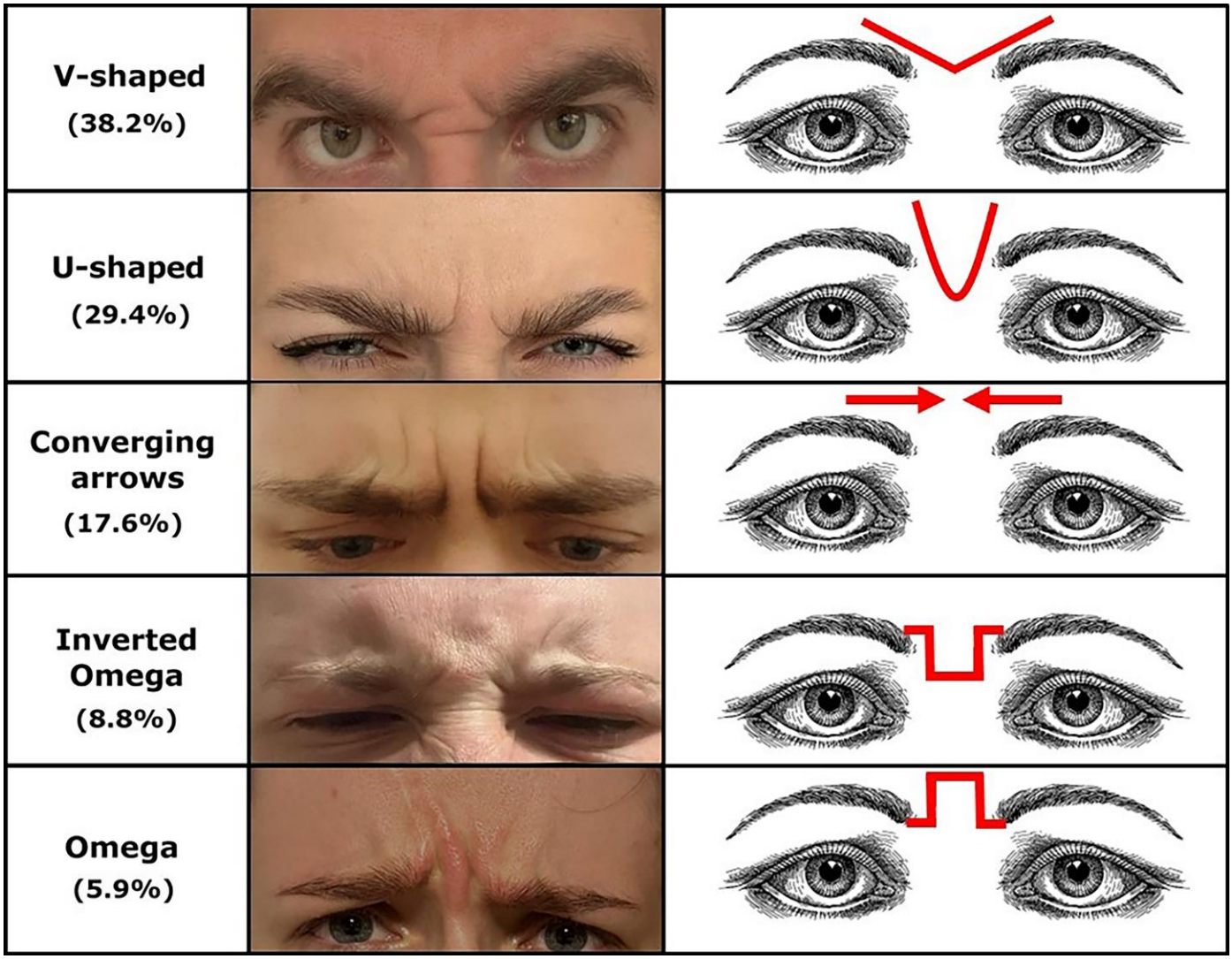

Figure 2. Distribution of the 5 glabellar contraction patterns in the study participants included in our study. Clinical photographs legend: V-shaped—healthy 27-year-old male; U-shaped—healthy 28-year-old female; converging arrows—healthy 25-year-old male; inverted omega—healthy 25-year-old male; omega—healthy 27-year-old female.

are presented for the entire sample in the tables, whereas data are presented stratified by sex in the "Results" section.

RESULTS

General Description

Thirty-four healthy young individuals of Caucasian Polish descent were investigated (17 females and 17 males) with a mean age of 23.6 (2.4) years [range: 20-30] and a mean BMI of 22.8 (2.4) kg/m^2 [range: 18.6-27.8].

The glabellar contraction pattern distribution was V-shaped $n = 13$ (38.2%); U-shaped $n = 10$ (29.4%); converging arrows $n = 6$ (17.6%); inverted omega $n = 3$ (8.8%); and omega $n = 2$ (5.9%) (Figure 2).

Descriptive Muscle Parameters

Procerus Muscle (PM)

The average length of the PM was 25.76 (3.2) mm in females vs 26.05 (4.2) mm in males, with $P = .818$ for sex differences. The values for PM thickness and width were (female/male) 0.83 (0.2) mm/1.15 (0.3) mm and 26.85 (4.8) mm/28.59 (3.7) mm, with $P < .001$ and $P = .250$ for sex differences, respectively (Figure 3).

Corrugator Supercilii Muscle (CSM)

The average length of the CSM was 23.19 (3.0) mm in females, whereas in males it was 25.38 (3.8) mm, with $P = .073$ for sex differences. The respective values for average thickness and width in females/males were 0.76 (0.1) mm/1.02 (0.2) and 7.87 (0.7) mm/8.94 (0.8), with $P < .001$ and $P < .001$ for sex differences, respectively (Figure 4).

Orbicularis Oculi Muscle (OOM)

The OOM average surface area was 3133 (382) mm^2 in females, whereas in males it was 3137 (398) mm^2, with $P = .978$. The average OOM thickness was 0.82 (0.1) mm in females, whereas in males it was 1.02 (0.2) mm, with $P < .001$. The average OOM height and width were in females/males 59.50 (4.8) mm/59.20 (4.8) mm and 66.91 (4.4) mm/67.58 (5.4) mm, with $P = .855$ and $P = .695$, respectively (Figure 5).

Frontalis Muscle (FM)

The average FM length was 49.64 (6.3) mm in females, whereas in males it was 70.57 (7.2) mm, with $P < .001$. The average thickness

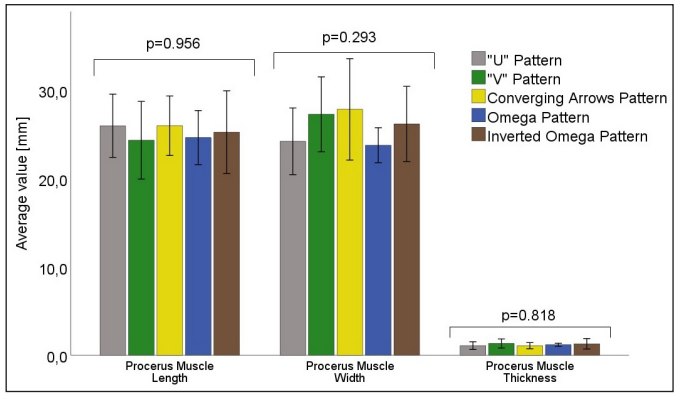

Figure 3. The average values in millimeters (mm) for each glabellar contraction type for the procerus muscle (PM) length, width, and thickness. Probability values (*P* values) from across-group testing were calculated by analysis of variance (ANOVA).

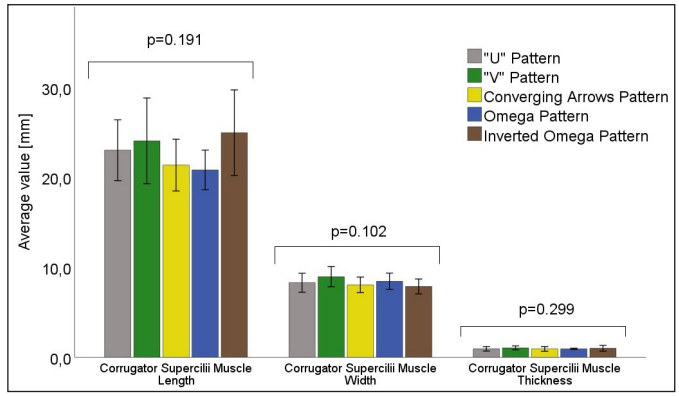

Figure 4. The average values in millimeters (mm) for each glabellar contraction type for the corrugator supercilii muscle (CSM) length, width, and thickness. Probability values (*P* values) from across-group testing were calculated by analysis of variance (ANOVA).

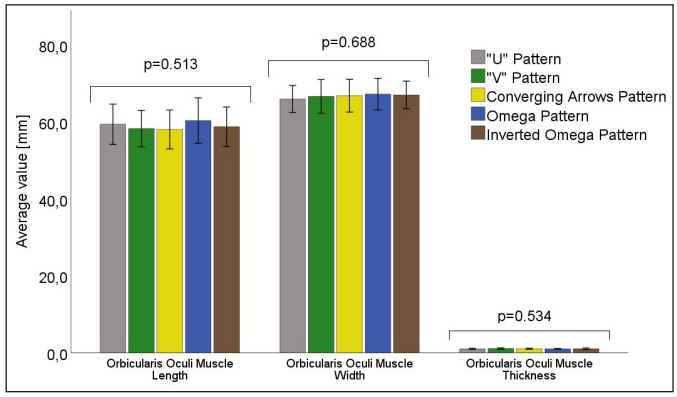

Figure 5. The average values in millimeters (mm) for each glabellar contraction type for the orbicularis oculi muscle (OOM) height, width, and thickness. Probability values (*P* values) from across-group testing were calculated by analysis of variance (ANOVA). (Surface area not shown).

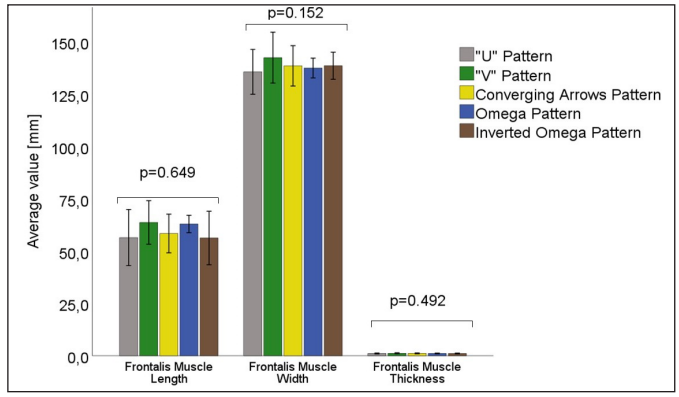

Figure 6. The average values in millimeters (mm) for each glabellar contraction type for the frontalis muscle (FM) length, width, and thickness. Probability values (*P* values) from across-group testing were calculated by analysis of variance (ANOVA).

and width in females/males were 0.94 (0.2) mm/1.11 (0.2) mm and 134.2 (8.7) mm/144.0 (11.1) mm, with $P = .016$ and $P = .007$, respectively (Figure 6). Values for the investigated muscle parameters stratified by glabellar contraction pattern are provided in Table 1 along with *P* values for across-group comparisons (Table 1).

Multivariate Analyses

To identify the influence of the various muscle parameters on the distribution of the 5 glabellar contraction patterns, multinomial logistic regression models were calculated. Age, sex, and BMI were included in the model because it is known that these factors can influence skin wrinkle formation alongside the respective muscle variables of interest. With the exception of frontalis muscle length ($P = .022$), none of the investigated muscle parameters displayed a statistically significant influence on the distribution of the glabellar contraction pattern, with all $P > .05$. For detailed information on each muscle parameter please see Table 2.

DISCUSSION

The present study was conducted to provide scientific validity for previously proposed treatment recommendations based on the respective underlying glabella musculature in a cohort of neuromodulator-naive patients.[5] The assessment of glabellar skin rhytids in our study sample confirmed the presence of typical patterns, in line with the publication of de Almeida et al.[5] However, the identified glabellar contraction type distribution in the present study was different when compared to the initial publication, with the most frequent type being the V-shaped pattern (38.2%) and the least frequent being the omega pattern (5.9%). This discrepancy was likewise noted by Kim et al, Kamat et al, Jiang et al, and Hsieh et al, which could be due to differences in ethnic backgrounds of the investigated cohorts: Korean vs Indian vs Chinese vs Polish Caucasian vs Brazilian.[6-9] This variation most likely indicates that factors other than muscular anatomy may play a role in the formation of glabellar rhytids.

It may be helpful to review the formation of glabellar rhytids in this context: glabellar muscles originate all together from bony features and either connect directly to the skin (CSM, PM) or fuse with other periorbital muscles to form muscle complexes (PM, OOM, FM).[11-13] Under contraction, these muscles move the skin in the direction of their longitudinal axis and cause skin folds that are oriented perpendicular to the muscle fiber orientation: horizontal forehead lines during FM contraction, horizontal glabellar lines during PM contraction, vertical glabellar lines during CSM contraction, lateral canthal lines during OOM contraction.[14,15]

However, the probability of forming a fold and its location is influenced by the stability of the overlying soft tissues, which is influenced

Table 1. Muscle Parameters Stratified By Glabellar Contraction Pattern, Mean (SD)

	U-shaped	V-shaped	Converging arrows	Omega	Inverted omega	*P* value by ANOVA
PM length, mm	26.59 (3.3)	25.48 (4.4)	25.95 (3.9)	24.78 (0.3)	26.10 (3.9)	.956
PM thickness, mm	0.93 (0.2)	1.01 (0.3)	0.95 (0.2)	1.05 (0.3)	1.16 (0.7)	.818
PM width, mm	26.03 (4.0)	29.07 (3.4)	29.45 (7.0)	25.49 (0.9)	25.50 (1.7)	.293
CSM length	23.49 (1.5)	25.54 (4.2)	22.46 (3.4)	21.87 (0.9)	26.80 (5.3)	.191
CSM thickness	0.86 (0.2)	0.97 (0.2)	0.77 (0.1)	0.94 (0.1)	0.84 (0.2)	.299
CSM width	7.96 (0.7)	8.93 (0.9)	8.08 (1.0)	8.53 (0.1)	8.24 (0.9)	.102
OOM surface area, mm^2	3126 (307)	3165 (383)	3134 (448)	3168 (84)	3015 (198)	.977
OOM thickness	0.85 (0.2)	0.98 (0.2)	0.92 (0.1)	0.92 (0.1)	0.92 (0.2)	.534
OOM height, mm	59.73 (4.4)	58.78 (4.6)	60.10 (4.6)	63.64 (8.3)	56.20 (2.0)	.513
OOM width	66.57 (2.7)	68.50 (5.4)	66.30 (7.1)	63.82 (6.7)	68.41 (2.7)	.688
FM length	56.69 (15.1)	63.63 (11.3)	58.59 (11.5)	65.46 (4.4)	55.63 (15.6)	.649
FM thickness	0.92 (0.2)	1.06 (0.2)	1.09 (0.3)	1.01 (0.1)	1.08 (0.1)	.492
FM width	134.4 (9.5)	145.1 (11.6)	137.9 (10.6)	134.8 (1.7)	134.6 (9.5)	.152

Unadjusted probability value is provided by 1-way analysis of variance (ANOVA) to identify differences across glabellar contraction patterns. CSM, corrugator supercilii muscle; FM, frontalis muscle; OOM, orbicularis oculi muscle; PM, procerus muscle; SD, standard deviation.

Table 2. Multinomial Regression Analyses of Age, Sex, BMI, and Muscle Parameters

	Age *P* value	Sex *P* value	BMI *P* value	Muscle variable *P* value
PM length	.870	.040*	.319	.939
PM thickness	.725	.019*	.337	.326
PM width	.980	.056	.250	.311
CSM length	.679	.023*	.121	.095
CSM thickness	.798	.427	.212	.760
CSM width	.913	.236	.330	.501
OOM area	.838	.036*	.193	.816
OOM thickness	.862	.022*	.247	.216
OOM height	.824	.041*	.173	.295
OOM width	.921	.040*	.284	.723
FM length	.456	.004*	.274	.022*
FM thickness	.874	.015*	.226	.182
FM width	.893	.093	.137	.152

Age, sex, BMI, and the respective muscle parameter are covariates, and the distribution of the glabellar contraction type is the dependent variable. Statistically significant values are highlighted with an asterisk ($P \leq .05$). BMI, body mass index; CSM, corrugator supercilii muscle; FM, frontalis muscle; OOM, orbicularis oculi muscle; PM, procerus muscle.

by dermal thickness, dermal stability, subdermal fatty layer thickness, and collagen network firmness located within the superficial fatty layer (like the suprafrontalis fascia of the forehead).[16-18] These factors oppose wrinkle formation and can therefore dictate if and where a fold is formed; see the transition of wrinkles from dynamic to static. An example to consider is the creases of shoes: each shoe develops creases after a certain time in use and each shoe has a different pattern, depth, and number of creases. This shoe-specific crease pattern however does not depend on the foot inside that causes the movement but rather on the material composition of the shoe. In other

words, the same foot can cause different crease patterns depending on which shoes are worn.

Translating this into a glabellar contraction pattern, it can be argued that the underlying glabellar musculature is primarily constant in origin and insertion (the foot), whereas the overlying soft tissue envelope (the shoe) may be influenced by various factors such as age, sex, BMI, etc. The resulting glabellar contraction pattern might not be the result of variable glabellar muscular anatomy but rather the result of a combination of factors that affect the surrounding soft tissue envelope. Assuming that variations in the shape of glabellar skin rhytids are solely related to the underlying muscular anatomy may mislead clinicians into following neuromodulator algorithms that provide minimal to no clinical benefit.

Comparing the length, width, and thickness of the procerus, corrugator supercilii, orbicularis oculi, and frontalis muscles, unadjusted models revealed that there was no statistically significant difference between the 5 glabellar contraction types. This indicates that independent of the skin rhytid pattern, the underlying musculature was not different between the investigated groups in this sample for the measured parameters, with all $P \geq .102$ (Table 1). Adjusting for age, sex, and BMI revealed that only 1 parameter (FM length) displayed a statistically significant influence on the glabellar contraction pattern (Table 2). However, this outcome was most likely related to the influence of sex, because male study participants had an average FM length of 70.57 (7.2) mm, whereas females had an average FM length of 49.64 (6.3) mm, with $P < .001$. It must be noted that after conducting Bonferroni adjustment for multiple testing (0.05 divided by 13 tests conducted led to a new probability level of $P \leq .004$) the FM length would likewise lose its statistical significance. The most influential factor in this study seemed to be sex, because direct comparisons between male and female study participants showed in general higher values for males than for females. The absence of statistical significance of age and BMI in the conducted analyses is most likely the consequence of the homogenous study sample which had an age range of 20 to 30 years and a BMI range of 18.6 to 27.8 kg/m^2.

Support for the results obtained comes from the aesthetic injector community, which indicated in a blinded survey that treatment of the glabella presents the least perceived difficulty for obtaining a perfect aesthetic outcome when compared to all other facial regions.[3] This is most likely attributed to the fact that, independent of a skin contraction pattern, the underlying glabellar musculature can be repeatedly and precisely targeted by following approved algorithms. Adjusting neuromodulator administration points according to a skin rhytid pattern may result in adverse events or reduced effectiveness for the patient. This is especially true because a glabellar neuromodulator treatment targets glabellar muscles for skin rhytid reduction. Some examples of clinical consequences resulting from injecting in other than the FDA-approved injection sites are the following: (1) injecting too high into the forehead can affect the eyebrow elevation segment of the frontalis muscle and result in eyebrow ptosis; (2) medializing the injection algorithm may have less effect on the most lateral frontalis muscle fibers, resulting in a “Spock” eyebrow formation; and (3) targeting the glabella in a location higher than the level of the eyebrows may result in medial eyebrow ptosis and cause an angry facial expression.[12,19-26]

This study, however, is not free of limitations. First, the study sample was relatively small, with $n = 34$ patients. A larger sample would have been favorable for the statistical tests conducted. (It should be noted that this study did not receive any funding support but instead was carried out with the help of the involved departments and authors.) Second, the slice thickness of the MR imaging procedures was 0.9 mm, which may have resulted in inaccuracies during the conducted measurements. Here it must be stated that for the measurements conducted, average values were obtained for muscle length, width, and thickness, which allows for the accounting of smaller measurement errors. Third, only study patients of Polish Caucasian origin were included. The results may differ if another sample is investigated, and future studies will need to address the limitations mentioned and expand on the results presented here. Future studies could incorporate ultrasound-based investigations to measure dermal or full soft tissue thickness, cutometry could be utilized to measure dermal elasticity or dermal stiffness, and electromyographic analyses could be conducted to determine baseline and contraction muscle tone to increase understanding of the results presented in this study.

Despite the absence of a clinical investigative study arm to confirm or disprove the assumptions made regarding clinical outcome, our results indicate a potential trend: glabellar muscles parameters as evaluated by MRI (such as length, width, thickness, surface area) do not statistically significantly influence the distribution of glabellar contraction patterns (Tables 1, 2, Figures 3-6).

CONCLUSIONS

The results of this study reveal that, based on the MRI parameters investigated and the investigated cohort, there does not appear to be a strong relationship between glabellar contraction patterns and underlying glabella muscle anatomy. Utilizing glabellar contraction patterns to design neuromodulator treatment algorithms may be of variable clinical merit. Future investigations will be needed to confirm and expand on the results presented here. In particular, clinical trials with an interventional study arm may help to evaluate any potential relationship in more depth.

Disclosures

The authors declared no potential conflicts of interest with respect to the research, authorship, and publication of this article.

Funding

The authors received no financial support for the research, authorship, and publication of this article.

REFERENCES

1. Aesthetic Plastic Surgery National Databank Statistics 2022. *Aesthet Surg J*. 2023;43(Suppl 2):1-19. doi: 10.1093/asj/sjad354
2. International Society of Aesthetic Plastic Surgery. ISAPS international survey on aesthetic/cosmetic procedures performed in 2022. Accessed August 28, 2024. https://www.isaps.org/discover/about-isaps/global-statistics/global-survey-2022-full-report-and-press-releases/
3. Cotofana S, Mehta T, Davidovic K, et al. Identifying levels of competency in aesthetic medicine: a questionnaire-based study. *Aesthet Surg J*. 2024;44:1105-1117. doi: 10.1093/asj/sjae096
4. Cotofana S, Solish N, Gallagher C, Beleznay K, Hernandez CA, Bertucci V. The anatomy behind eyebrow positioning: a clinical guide based on current anatomic concepts. *Plast Reconstr Surg*. 2022;149:869-879. doi: 10.1097/PRS.0000000000008966
5. de Almeida AR, da Costa Marques ER, Banegas R, Kadunc BV. Glabellar contraction patterns: a tool to optimize botulinum toxin treatment. *Dermatol Surg*. 2012;38(9):1506-1515. doi: 10.1111/j.1524-4725.2012.02505.x
6. Kim HS, Kim C, Cho H, Hwang JY, Kim YS. A study on glabellar wrinkle patterns in Koreans. *J Eur Acad Dermatol Venereol*. 2014;28:1332-1339. doi: 10.1111/jdv.12286
7. Kamat A, Quadros T. An observational study on glabellar wrinkle patterns in Indians. *Indian J Dermatol Venereol Leprol*. 2019;85:182-189. doi: 10.4103/ijdvl.IJDVL_211_17

8. Jiang H, Zhou J, Chen S. Different glabellar contraction patterns in Chinese and efficacy of botulinum toxin type a for treating glabellar lines: a pilot study. *Dermatol Surg*. 2017;43:692-697. doi: 10.1097/DSS.0000000000001045
9. Hsieh DM, Zhong S, Tong X, et al. A retrospective study of Chinese-specific glabellar contraction patterns. *Dermatol Surg*. 2019;45:1406-1413. doi: 10.1097/DSS.0000000000001808
10. Rams DJ, Alfertshofer M, Batko J, et al. Investigating the contraction pattern of the zygomaticus major muscle and its clinical relevance: a functional MRI study. *Aesthetic Plast Surg*. 2024;48:2722-2729. doi: 10.1007/s00266-024-03876-8
11. Abramo AC, Do Amaral TP, Lessio BP, De Lima GA. Anatomy of forehead, glabellar, nasal and orbital muscles, and their correlation with distinctive patterns of skin lines on the upper third of the face: reviewing concepts. *Aesthetic Plast Surg*. 2016;40:962-971. doi: 10.1007/s00266-016-0712-z
12. Solish N, Bertucci V, Green JB, Kane MAC. Optimizing outcomes when treating glabellar lines. *Aesthet Surg J*. 2023;43:786-788. doi: 10.1093/asj/sjad087
13. Daniel RK, Landon B. Endoscopic forehead lift: anatomic basis. *Aesthet Surg J*. 1997;17:97-104. doi: 10.1016/S1090-820X(97)80070-2
14. Moqadam M, Frank K, Handayan C, et al. Understanding the shape of forehead lines. *J Drugs Dermatol*. 2017;16:471-477.
15. Cotofana S, Freytag DL, Frank K, et al. The bidirectional movement of the frontalis muscle: introducing the line of convergence and its potential clinical relevance. *Plast Reconstr Surg*. 2020:145;1155-1162. doi: 10.1097/PRS.0000000000006756
16. Alfertshofer M, Engerer N, Frank K, Moellhoff N, Freytag DL, Cotofana S. Multimodal analyses of the aging forehead and their clinical implications. *Aesthet Surg J*. 2023;43:NP531-NP540. doi: 10.1093/asj/sjad009
17. Shin JW, Kwon SH, Choi JY, et al. Molecular mechanisms of dermal aging and antiaging approaches. *Int J Mol Sci*. 2019;20:2126. doi: 10.3390/ijms20092126
18. Swift A, Liew S, Weinkle S, Garcia JK, Silberberg MB. The facial aging process from the "inside out". *Aesthet Surg J*. 2021;41:1107-1119. doi: 10.1093/asj/sjaa339
19. Zargaran D, Zoller F, Zargaran A, et al. Complications of cosmetic botulinum toxin a injections to the upper face: a systematic review and meta-analysis. *Aesthet Surg J*. 2022;42:NP327-NP336. doi: 10.1093/asj/sjac036
20. Cho ES, Hwang JY, Kim ST. A proposal to prevent the "Mephisto sign" side effect of botulinum toxin type a injection in chronic migraine. *Yonsei Med J*. 2013;54:1542-1544. doi: 10.3349/ymj.2013.54.6.1542
21. Fagien S, Raspaldo H. Facial rejuvenation with botulinum neurotoxin: an anatomical and experiential perspective. *J Cosmet Laser Ther*. 2007;9(Suppl 1):23-31. doi: 10.1080/17429590701523836
22. Kim SB, Kim HM, Ahn H, et al. Anatomical injection guidelines for glabellar frown lines based on ultrasonographic evaluation. *Toxins (Basel)*. 2021;14:17. doi: 10.3390/toxins14010017
23. Monheit G, Lin X, Nelson D, Kane M. Consideration of muscle mass in glabellar line treatment with botulinum toxin type A. *J Drugs Dermatol*. 2012;11:1041-1045.
24. Lorenc ZP, Smith S, Nestor M, Nelson D, Moradi A. Understanding the functional anatomy of the frontalis and glabellar complex for optimal aesthetic botulinum toxin type A therapy. *Aesthetic Plast Surg*. 2013;37:975-983. doi: 10.1007/s00266-013-0178-1
25. Cho Y, Lee HJ, Lee KW, Lee KL, Kang JS, Kim HJ. Ultrasonographic and three-dimensional analyses at the glabella and radix of the nose for botulinum neurotoxin injection procedures into the procerus muscle. *Toxins (Basel)*. 2019;11(10):560. doi: 10.3390/toxins11100560
26. Wu WT, Chang KV, Chang HC, et al Ultrasound imaging of the facial muscles and relevance with botulinum toxin injections: a pictorial essay and narrative review. *Toxins (Basel)*. 2022;14:101. doi:10.3390/toxins14020101